Redox-dependent formation of a viral amyloid and functional impact

Frank Gondelaud, Alexandre Lalande, Giulia Pesce, Christophe Bignon, Patrick Fourquet, Denis Ptchelkine, Nicolas Brouilly, Pierre-Yves Lozach, Denis Gerlier, Cyrille Mathieu, et al.

Redox-dependent formation of a viral amyloid and functional impact

Frank Gondelaud[1*†], Alexandre Lalande[2†], Giulia Pesce[1], Christophe Bignon[1], Patrick Fourquet[3], Denis Ptchelkine[1], Nicolas Brouilly[4], Pierre-Yves Lozach[5], Denis Gerlier[2], Cyrille Mathieu[2*] and Sonia Longhi[1*]

[1]Laboratoire Architecture et Fonction des Macromolécules Biologiques (AFMB), UMR 7257, Aix Marseille University and Centre National de la Recherche Scientifique (CNRS), 163 Avenue de Luminy, Case 932, 13288 Marseille, France

[2]CIRI, Centre International de Recherche en Infectiologie, Univ Lyon, Inserm, U1111, CNRS, UMR5308, Université Claude Bernard Lyon 1, Ecole Normale Supérieure de Lyon, 69007, Lyon, France

[3]INSERM, Centre de Recherche en Cancérologie de Marseille (CRCM), Centre National de la Recherche Scientifique (CNRS), Marseille Protéomique, Institut Paoli-Calmettes, Aix Marseille University, 27 Bvd Leï Roure, CS 30059, 13273 Marseille, France

[4]Aix Marseille Université, CNRS, IBDM, Marseille, France

[5]University of Lyon, INRAE, EPHE, IVPC (Infections Virales et Pathologie Comparée), 69007, Lyon, France

[†]Authors contributed equally to this work.
*Corresponding authors: sonia.longhi@univ-amu.fr; cyrille.mathieu@inserm.fr; frank.gondelaud@univ-amu.fr

Author Contributions: F.G., A.L., G.P., C.M. and S.L. designed the experiments; F.G. performed all the *in-vitro* experiments except for the mass spectrometry analyses that were performed by P.F.; A.L. performed transfection, live imaging microscopy studies and ROS quantification; C.B. and F.G. generated all the constructs except for the constructs of the W^{HeV} proteins with an N-terminal *tc* tag that were generated by A.L.; D.P. provided guidance on NS-EM studies; G.P. carried out the ultramicrotomy experiments and related EM analyses with the help and guidance of N.B.; D.G. provided guidance on transfection and confocal microscopy studies and suggested to perform experiments with FKBP; P.Y.L provided guidance on the use of the *tc* tag; F.G, A.L, G.P., P.F, C.M. and S.L analyzed the data; F.G. wrote the first draft of the manuscript and generated all the figures except for Figure 4 that was jointly generated by A.L., F.G. and G.P. and Figure 5 that was generated by A.L. and F.G.; F.G., A.L., C.M., D.G. and S.L generated the final version of the manuscript, and all the authors reviewed and edited it.

Competing interests: The authors declare no competing interest.

Keywords: Henipavirus, amyloid fibrils, innate immune response, cysteine, intrinsically disordered proteins

Abstract

The Hendra and Nipah viruses (HeV and NiV) are zoonotic biosafety level-4 pathogens within the *Paramyxoviridae* family. We previously showed that their W proteins form amyloid-like fibrils *in vitro*. Here, we demonstrate that W also forms fibrils *in cellula* and that cysteine residues are crucial in dictating the ability of W proteins to fibrillate. The cysteine oxidation state acts as a switch to generate either amorphous aggregates or flexible fibrils. Ectopic expression of W^{HeV} induces an oxidative stress and W^{HeV} fibrils were observed in the nuclei of different cell lines, with fibrillation being impaired by cysteine substitutions. Finally, nuclear fibrils are associated with an impairment of the NF-κB pathway in W^{HeV} transfected cells. This work provides experimental evidence for the ability of *Henipavirus* W proteins to fibrillate in transfected cells and the first clues on their functional impact.

Significance Statement

Nipah and Hendra viruses are severe pathogens infecting humans and livestock, classified among the 8 highest priorities for research by the WHO. The W protein, along with the V protein, is a virulence factor responsible for antiviral response inhibition and we demonstrate here that its fibrillation into amyloid-like fibrils occurs in the nucleus of transfected cells, with their formation being dependent of the redox state of the W cysteine residues. The sole transfection of W provokes the production of reactive oxygen species, creating a suitable environment for the fibrils to form. Finally, we show that W fibrils enhance the repression of the antiviral response, thus pointing to W fibrillation as a new promising antiviral target.

Introduction

Hendra (HeV) and Nipah viruses (NiV) are members of the *Henipavirus* genus, within the *Paramyxoviridae* family of the *Mononegavirales* order. They are zoonotic viruses responsible for severe encephalitis and respiratory illness with a high case fatality, and as such, they are considered high-priority targets by the WHO. Since the identification of HeV and NiV in humans and fruit-bats from the *Pteropus* genus (1, 2), new species have been described including the Cedar virus identified in bats (3), the Langya virus identified in patients, bats and shrews (4, 5) and two novel species in shrews (6). Transmission from bats to humans occurs through the consumption of raw date palm sap (NiV) or from close contact with infected livestock, particularly horses (HeV) and pigs (NiV) (7). Interhuman transmissions also occurred in the case of NiV Bangladesh strain (8). Henipavirus outbreaks are unpredictable but occur almost every year with a high case fatality rate (70-90%) while no antiviral therapeutic nor vaccine is currently available (1, 9). For these reasons, HeV and NiV are biosafety level-4 pathogens.

Henipaviruses, like all paramyxoviruses, are enveloped viruses containing a non-segmented single-stranded RNA genome of negative polarity (-ssRNA) tightly associated with the nucleoprotein (N). The encapsidated RNA is the template of the viral RNA-dependent RNA polymerase (L) that, in association with the phosphoprotein (P), ensures the transcription and the replication of the viral genome (1). Beyond the P protein, the P gene also drives the synthesis of the V, W, and C proteins. The V and W proteins are produced through a co-transcriptional editing mechanism involving the addition of one (V) or two (W) non-templated G nucleotides at the editing site of the P messenger (2). In NiV-infected cells, equimolar proportions of P, V, and W transcripts are detected in the early stage of infection while the quantity of V and W transcripts increases as the infection progresses (10). The W proteins of HeV and NiV contain a nuclear localization sequence (NLS) in their unique C-terminal domain (CTD) leading to their nuclear accumulation in infected cells. Nuclear importation relies on binding to importins α3 and α4 and, to a lower extent, to importin α1 and α7 (11). W, along with P and V, also contains a nuclear export signal (NES) in its N-terminal domain (NTD) ensuring its export to the cytoplasm of infected cells *via* a Crm-1-dependent nuclear export (12, 13). Inhibition of Crm-1 in transfected cells leads to the accumulation of NiV V in the nucleus demonstrating its dual localization despite its predominant localization in the cytoplasm in untreated cells (13). Since W is almost found in the nucleus of infected cells, the NLS overcomes the NES (10, 14).

The V and W proteins are virulence factors implicated in the inhibition of the antiviral response by binding several key cellular proteins (1, 10, 15–17). The lack of the V and W proteins in the non-pathogenic Cedar virus due to the absence of the RNA editing site, concomitantly to the absence of pathogenicity associated with this virus in humans further supports this view (3, 18). W proteins bind and sequester in the nucleus STAT1 through their NTD, common to P and V, inhibiting the interferon response (1, 16, 19). Additionally, the CTD of the W proteins binds 14-3-3 proteins through its serine 449 leading to 14-3-3 protein nuclear accumulation. This accumulation enhances the nuclear export of p65, reducing its ability to interact with its promoter targets, thereby inhibiting the NF-κB-induced proinflammatory response (20). Binding to 14-3-3 also provokes cell apoptosis through a less defined mechanism (21).

We previously showed that the W proteins from HeV and NiV (W^{HeV} and W^{NiV}) are intrinsically disordered and can aggregate in an amyloid-like fashion (22). W^{NiV} and W^{HeV} contain cysteine residues implicated in W dimerization (22). We hypothesized that cysteine residues could impact the fibrillation ability of W proteins. Using various biophysical approaches and site-directed mutagenesis, we demonstrate here that the cysteine oxidation state dictates the ability of W^{HeV} and W^{NiV} to fibrillate. We also show that W^{HeV} forms fibrils in the nucleus of transfected cells with the redox-dependance of the process being retained also in the cellular context. Finally, we shown that W fibrils enhance the repression of the NF-κB-mediated antiviral response, suggesting a role of W fibrils in viral escape from the innate immune response.

Results

Cysteines are responsible for the formation of oligomeric species and of a compact conformation

W^{HeV} and W^{NiV} contain four and six cysteine residues respectively, three of which are shared by both proteins (**Figure 1A**). Since the W proteins are intrinsically disordered (22) and thus possess a large solvent-accessible surface area, we hypothesized a strong reactivity of these residues. The proteins, purified in reducing and denaturing conditions, were incubated at 37°C in the presence of urea to avoid their spontaneous aggregation into amyloid-like fibrils while enabling cysteines to undergo natural oxidation, presumably *via* the formation of intra- and/or interchain disulfide bridges. This pre-incubation in urea of the proteins will thereafter be referred to as “oxidative preincubation” (**Supplementary Figure 1**).

In addition to the monomer (vertical violet line in **Figure 1B** and peak I in **Supplementary Figure 2A**), size exclusion chromatography (SEC) analysis of the W proteins during oxidative preincubation showed the fast formation of dimeric species (vertical yellow line in **Figure 1B**), consistent with previous observations (22), as well as the formation of higher-order oligomers within 24h for W^{HeV} and 48h for W^{NiV} (vertical grey line in **Figure 1B**). The nature of the oligomeric species of W^{HeV} was disentangled by mass photometry, which showed the co-existence in the sample of monomeric, dimeric, trimeric and likely tetrameric species (**Supplementary Figure 2B**). Additionally, a species (vertical pink line in **Figure 1B** and peak II in **Supplementary Figure 2A**) that eluted at a volume slightly larger than that of the initial monomeric species can be detected upon incubation. For W^{HeV}, non-reducing SDS-PAGE and mass spectrometry analysis revealed that this species corresponds to a monomeric form of the protein (**Supplementary Figures 2C** and **2D**), and its elution volume indicates a more compact conformation (**Figure 1B**).

While W^{HeV} oligomerization does not seem to evolve further after 48h of oxidative preincubation, in the case of W^{NiV} it continues to progress even after 4 days (**Figure 1B**). Addition of DTT during the preincubation in urea (for 72h for W^{HeV} and for 96h for W^{NiV}), led to the disappearance of both the oligomers (grey line in **Figure 1B**) and the compact conformation (pink line in **Figure 1B**) indicating

that they are both redox-sensitive and result from the formation of inter- and intramolecular disulfide bonds, respectively (**Figure 1B**).

Cysteine oxidation is required for W^{HeV} and W^{NiV} fibrillation

The aggregation of W^{HeV} and W^{NiV} was followed by turbidity as well as by means of thioflavin T (ThT) fluorescence measurements (**Figure 1C-F**). In these experiments, as well as in all the ensuing experiments unless differently stated, the W proteins were pre-incubated for different periods in urea to promote the formation of oligomers as in **Figure 1B**. After this oxidative preincubation period, urea was removed and the aggregation process was monitored for 2 hours at 37°C in a urea-free buffer (see procedure in **Supplementary Figure 1**). Urea removal without an oxidative preincubation, *i.e.* at time 0, led to the formation of macroscopically visible insoluble aggregates (**Figure 1C** and **1D**) that eventually sedimented and that did not bind ThT (**Figure 1E** and **1F**). By contrast, oxidative preincubation of W proteins for at least 24h led to a clear solution (**Figure 1C** and **1D**) containing species that bind ThT (**Figure 1E** and **1F**), suggesting the formation of fibrillar structures. After one or two additional preincubation days (48h and 72h in **Figures 1C** and **1E**), neither the turbidity nor the fluorescence emission evolved significantly for W^{HeV}, coincidentally with the arrest of oligomerization as observed by analytical SEC (**Figure 1B**). In contrast, W^{NiV} ThT binding continued to gradually increase (**Figure 1F**), mirroring the evolution of its oligomerization (**Figure 1B**). The nature of the aggregates formed with or without an oxidative preincubation period was assessed by negative-staining electron microscopy (NS-EM). Grids were prepared after the 2 hours of incubation over which the aggregation measurements were carried out (**Figure 1G**). The insoluble aggregates that are formed without an oxidative preincubation have an amorphous nature, while W^{HeV} and W^{NiV} preincubated in oxidative conditions give rise to amyloid-like fibrils (**Figure 1G**).

The constant increase of W^{NiV} oligomers content over time can be ascribed to its higher content in cysteine residues that keep reticulating the protein. The balance between fibril nucleation and elongation is low in the case of W^{HeV}, as judged from the fact that it rapidly forms fewer, though longer fibrils than W^{NiV}. On the contrary, the cysteine residue oxidation degree strongly promotes the extent of W^{NiV} nucleation which eventually forms massive amounts of short fibrils as shown by NS-EM (**Figure 1G**). The ThT fluorescence intensity seems to correlate with the nucleation extent rather than with fibril size.

W^{NiV} and W^{HeV} fibrils have the particularity of being not straight but rather highly curved (**Figure 1G**). Measurements of the contour length of W^{HeV} fibrils observed in micrographs revealed that 24h of oxidative incubation led to the longest fibrils, up to 830 nm in these experimental conditions, with an average size of 273 nm (**Figure 1H**). The proportion of short fibrils increased with the incubation time, presumably reflecting fibril fragmentation that regularly occurs in amyloid fibrils. After 72h of incubation, the average length of fibrils dropped to 179 nm (**Figure 1H** and **Supplementary Table 1**).

Taken together, these observations suggest that disulfide bonds formation is the initial step in the fibrillation of both W^{HeV} and W^{NiV} proteins, since non-oxidized monomeric species are poorly able to undergo fibrillation. We thus hypothesized that the oligomers could promote the formation of fibrillar structures. This was explored further by focusing on W^{HeV} in light of its lower cysteine content and its faster oligomerization compared to W^{NiV}. Since 48h of incubation of W^{HeV} represents a good compromise between solubility and fibril length, and because the oligomerization process does not progress further after this period, this oxidative preincubation time was selected for the following analyses of W^{HeV} fibrillation.

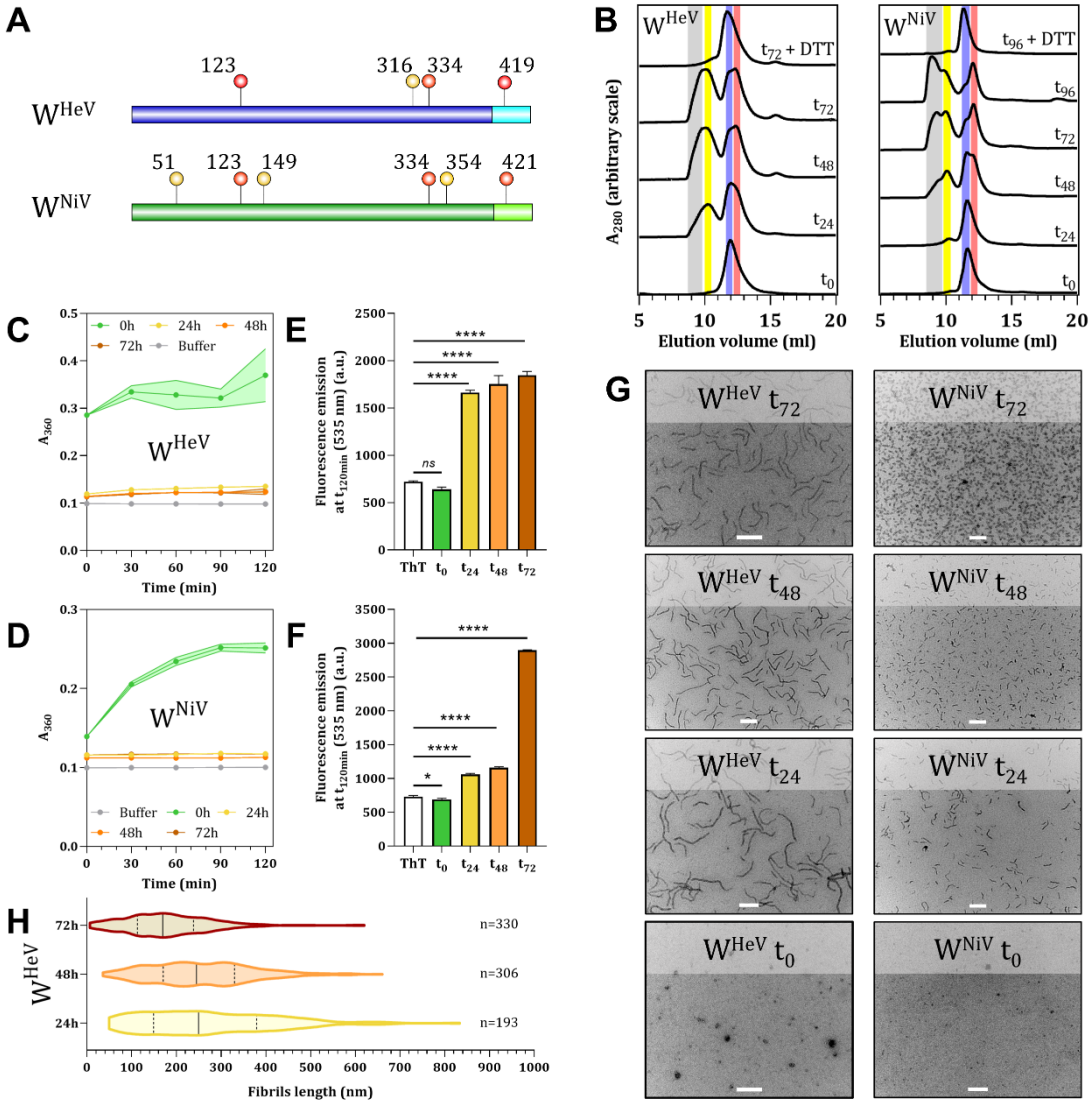

Figure 1: Cysteine residues oxidation of W^{HeV} and W^{NiV} is required to promote their fibrillation. A) Location of cysteine residues in W^{HeV} (blue) and W^{NiV} (green) proteins. Conserved Cys are indicated in red. Dark colors: N-terminal domain (NTD), bright colors: C-terminal domain. Schemes have been made with IBS software (23). **B)** Analytical SEC of the W proteins after different preincubation times in oxidative condition at 37°C in the presence of urea, and either in the absence (t_0, t_{24}, t_{48}, t_{72}, and t_{96}) or in the presence of DTT (t_{72} or t_{96} + DTT). The vertical grey, yellow, and violet bars correspond to the oligomeric, dimeric and monomeric species, respectively. The vertical pink bar corresponds to the more compact monomeric form. **C)** Turbidity and **E)** ThT fluorescence measurements of W^{HeV} preincubated for 0 (green), 24 (yellow), 48 (orange), and 72 hours (brown) at 37°C in urea and then buffer exchanged to remove urea. Shown is also the fluorescence of ThT alone (white). Panels C and D show the average values and s.d. as obtained from n=4 independent measurements. Statistical analysis was made with a one-way ANOVA, Dunnett's test, ns: not significant, ****: $p<0.0001$. The shaded region in C) corresponds to the error bar. **D)** Turbidity and **F)** ThT fluorescence measurements of W^{NiV} preincubated or not. The legend is the same as for C) and D). **G)** NS-EM micrographs of W^{HeV} and W^{NiV} incubated for 120 min at 37°C in urea-free buffer without preincubation (0h) or following a preincubation of 24, 48 and 72h at 37°C in urea. **H)** W^{HeV} fibril contour length measurements from NS-EM micrographs after 24, 48, and 72h of preincubation. Median and quartiles are represented as continuous and dotted lines, respectively. The number of fibril length measurements is indicated for each condition. Scale bar: 200 µm.